A NON-INVASIVE BEAM MONITOR FOR HADRON THERAPY BEAMS*

T. Cybulski #, C.P. Welsch, Cockcroft Institute / University of Liverpool, UK
A. Kacperek, B. Marsland, I. Taylor, A. Wray, Clatterbridge Cancer Centre, Wirral, UK
T. Jones, ASTeC, UK

Abstract

Hadron therapy allows for precise dose delivery to the tumour volume only, and hence decreases the dose delivered to the nearby organs and healthy tissue. Ideally, the beam would be monitored whilst being delivered to the patient. A novel, real–time and non-interceptive beam monitor for hadron therapy beams has been developed in the QUASAR Group. It is based on the LHCb VErtex LOcator (VELO) detector and couples to the treatment beam's transverse halo to determine the intensity, position and ultimately the dose of the treatment beam. This contribution presents the design of a stand-alone version of the VELO detector which was developed for the Clatterbridge Cancer Centre (CCC) treatment line. The mechanical and electronic design of the monitor and its data acquisition system are shown, with a focus on the detector positioning and cooling system.

INTRODUCTION

A non-invasive beam current monitor based on the multi-strip silicon LHCb VELO detector is being developed at the Cockcroft Institute/University of Liverpool and first tests at the treatment beam line at CCC are scheduled for October 2013. Initially, quadrupole variation scans were performed in October 2012 and followed by beam dynamics studies for beam 'halo' propagation [1]. Whilst having been originally designed to track vertices in the LHCb experiment at CERN [2], the flexible VELO architecture allows for different applications.

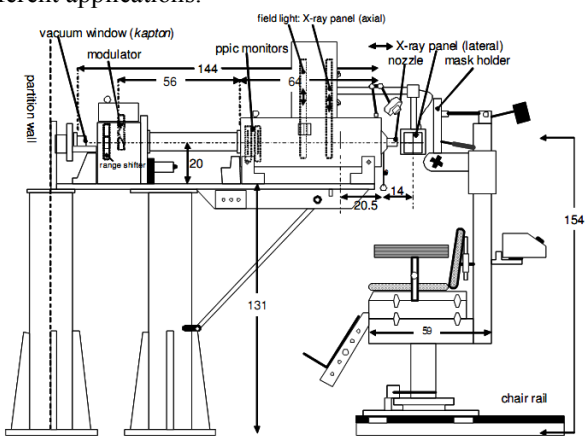

Figure 1: The treatment beam line layout at the Clatterbridge Cancer Centre [3].

*Work supported by the EU under contract PITN-GA-2008-215080 and the STFC Cockcroft Institute Core Grant No. ST/G008248/1
#t.cybulski@liverpool.ac.uk

First feasibility tests were performed at the treatment beam line in 2010 and demonstrated the possibility of non–intrusive beam monitoring [4]. These initial measurements consisted of data taken at several points along the propagation direction of the beam, starting from the brass collimator, see Fig. 1. A new method was proposed to relate the proton 'halo' region hit rate measured by the VELO detector with the absolute beam current provided by a Faraday cup (FC) and thereby get an indication of the dose delivered to the patient. The FC design was optimised using the FLUKA code [5] to maximise the charge collection efficiency for a 60 MeV proton beam.

LHCB VELO DETECTOR

The LHCb VELO detector is designed to track vertices originating in head-on collisions in the LHCb experiment. It uses the polar coordinate system defined by two semi-circular silicon sensors, see Fig. 2. Each sensor embeds 2048 diode strips resolving the position of the hit in r – and φ-coordinate. The applied silicon technology consists of n+ strips on n base substrate, which increases its radiation hardness. The r – measuring side is divided into four 45° sections, thus lowering the overall strip capacitance and occupancy [6][7]. The φ – side consists of inner- and outer- section of radially oriented strips with a skew angle being introduced between the regions to support the ghost hit recognition algorithms.

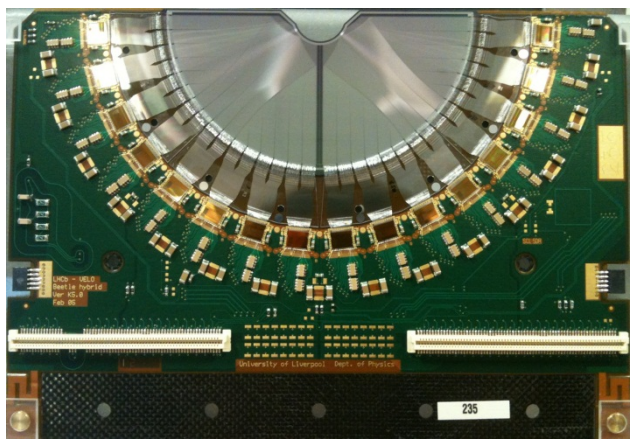

Figure 2: The LHCb VELO detector module consists of a semi-circular silicon detector (r-side in the picture) and front-end electronics – 16 Beetle chips located around the circumference of the sensor.

The design of the central part of the sensor lets the LHC beam pass without disturbing it, and most of all avoiding its interference with the detector. Therefore, the data collection is limited only to the product of the collisions.

ISBN 978-3-95450-127-4

The detector readout electronics works in synchronism with the LHC bunch crossing frequency at f_{LHC}=40 MHz. 16 Beetle chips read out the signal from the sensors. Their design allows to store the signal in a pipeline and thus to down grade the readout frequency to 1.1MHz (900ns readout time). The sampling rate of the detector is around 1.5 times higher than the RF frequency of the Scanditronix MC-60 cyclotron at CCC, where fc=25.7 MHz. This requires the development of dedicated software to readout and analyse the experimental data.

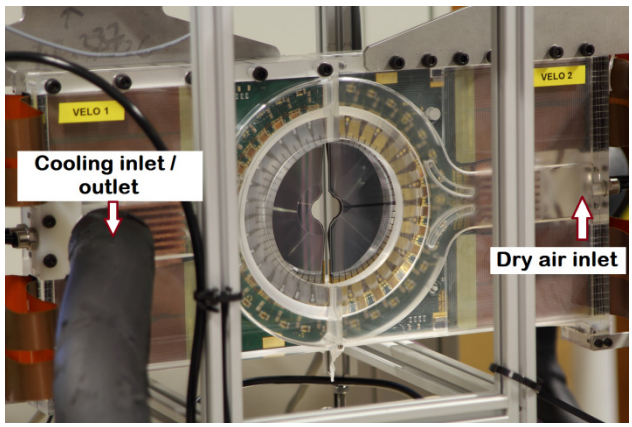

Figure 3: The LHCb VELO detector integration into the beam line at the CCC. The free drift space is housing a motorised stand with two VELO detector modules covering 2π azimuthal angle.

VELO INTEGRATION AT CCC

During normal operation the LHCb VELO detector works in vacuum. Its integration into the CCC treatment beam line, however, requires it to work in a different environment, namely in air. The designated integration area is between the modulator and ppie monitors, see Fig. 1 and Fig 3. Therefore, a designated stand was designed and manufactured to enable precise detector module positioning both, in the beam propagation direction (z) and the perpendicular axes. Three MacLennan stepper motors drive translation stages of the system with 5µm resolution in both axes, consecutively with 20000 steps / rotation in the z direction and 10000 steps / rotation in the perpendicular axes. The motors are powered by three independent Applied Motion ST5-Q motor drivers using Q and SCL host commands for communication, which have been utilised in developing a dedicated LabVIEW interface for driving all three axes both in an independent or coupled manner. The interface also puts limits on a few parameters, such as acceleration rate and speed, to avoid steps jumping during the movement caused by the weight of the modules, auxiliary electronics and mechanical elements. This ensures a high degree of repeatability of the detector positioning. The acceleration rate limit is set to 2 mm/s^2 and the speed to 5mm/s, which is just half of the nominal speed. The position of the motor gets reset in the memory of the driver at each power off. Therefore, the interface operation requires limit calibration independently for every axis on start up.

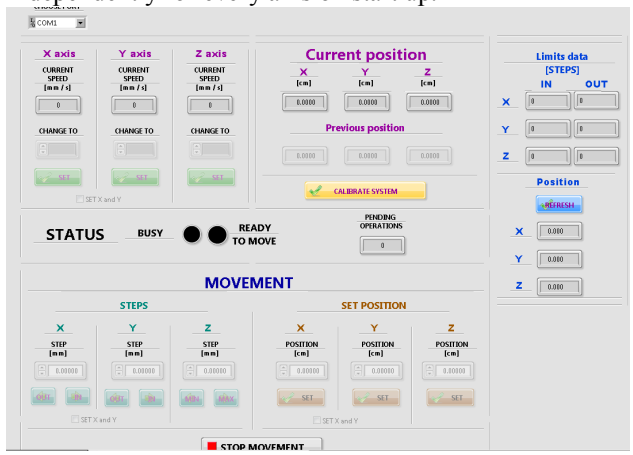

Figure 4: LabVIEW interface for driving the three axis motor system at CCC.

The movement range along the z axis allows setting the position from 0 to 20 cm, and 0 to 9.4cm in perpendicular direction. This gives access to precise proton 'halo' maps determination in the predicted region.

The LHCb VELO electronics was simplified for the purpose of the 'halo' studies, see Fig. 5. The repeater boards are not equipped with the Experiment Control System cards, which manage some of the interlocks and timing of the experiment. Also, long tail Kapton cables used in the experiment at LHC got replaced by short 33 cm short tail Kapton cables with dummy cards feeding the signal from the VELO hybrid to the ribbon cables and repeater boards in the next step. The ribbon cables are 4 times longer than in normal operation and measure 40 cm to allow flexible coupling between the moving translation stages and immobilised repeater boards.

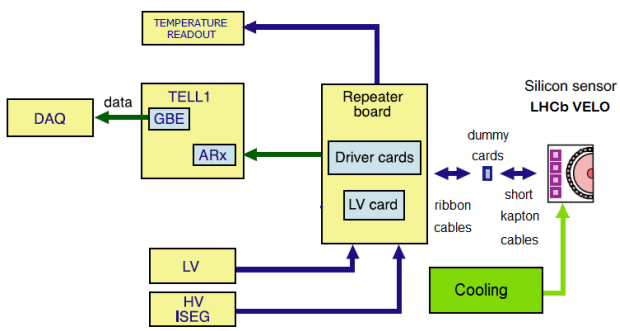

Figure 5: LHCb VELO electronics layout.

An ISEG EHS 82 05P-F-XXX PS supplies the reverse bias voltage to the silicon sensors with a ripple of 5 mVp-p at the maximum load of -500V [8]. The full depletion voltage, however, at this stage of the experiment does not exceed -80V. The power supply is also equipped with both positive and negative polarisation

ISBN 978-3-95450-127-4

channels, 4 channels of each type, being versatile to work with both n-in-n and p-on-n module technologies.

The low voltage card distributes power to the repeater boards and the VELO hybrids. Powering the read out chips produces 45 to 55W heat load and therefore the detector integration became challenging in meeting all three following requirements: dissipating the energy produced by the chips, keeping the silicon sensors in the temperature range between -7 and 0 degrees Celsius to lower the leakage current and radiation damage, and ultimately, keep the detector dry to prevent any damage to the electronics. Thus, purpose-built dry air shrouds were introduced to the set up to fulfil the above requirements and provide the mechanical support structure for the detector, see Fig. 6.

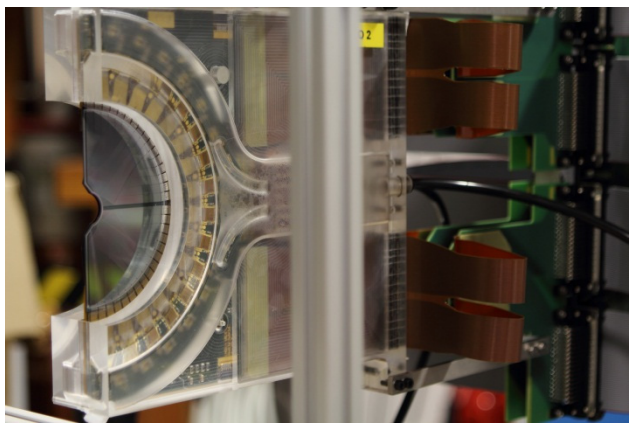

Figure 6: Dry air shrouds provide the mechanical support for the detector and constitute a border between its electronics embedded in dry air and ambient atmosphere.

The Thermo-Pyrolytic-Graphite central base of the hybrid couples directly to the cooling element. An ATC K3 chillier, with a cooling capacity of 3,200W, is capable of keeping the fully powered detector at a temperature of 0 degrees Celsius in its centre. Currently, the chillier is unable to provide sufficient coolant at lowest nominal temperature of -30 degrees. This is subject to further investigation and it is planned to test different cooling fluids with lower viscosity.

Due to the operation of the detector at temperatures lower than the dew point of ambient air, dry air shrouds constitute a barrier between the detector electronics and atmosphere. Dry air from a BAMBI VTS75D compressor gets injected between the detector and the Perspex shroud with an efficiency of approx. 90 l/min at a pressure of slightly more than 1bar. This, however, has turned out to be insufficient to protect the whole area of the silicon sensor and therefore higher air throughput options are being considered at the moment.

Initial performance tests of the detector in a laboratory environment under atmospheric pressure and without any additional electromagnetic screening showed very good agreement with data collected at the commissioning stage of each module during their production. The noise level at a bias voltage of -100V is, as expected, at the level of 2 – 3 analogue to digital counts (ADCs), see. Fig. 7.

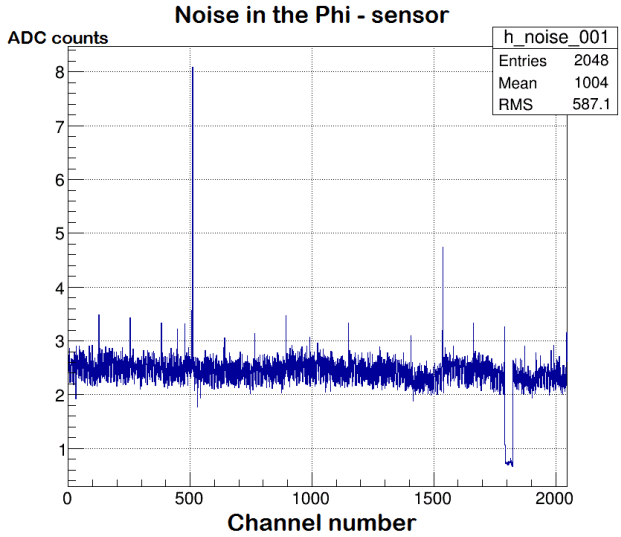

Figure 7: Noise level recorded 1000 trigger events for the φ-sensor on the hybrid No. 130.

A dedicated alignment system was built to match the detector z axis with the centre of the beam. Two cross–shaped targets, placed at both ends of the stand, mark the centre of the silicon sensors. A cylindrical boss fitted on the beam pipe houses a laser, which simulates the beam centre in the beam propagation direction, see Fig. 8. Alignment is then achieved when images of both targets match on a screen placed behind the last target. Additionally, the position can be verified against the absolute treatment isocentre, corresponding to the centre of the X-ray panel, see Fig. 1.

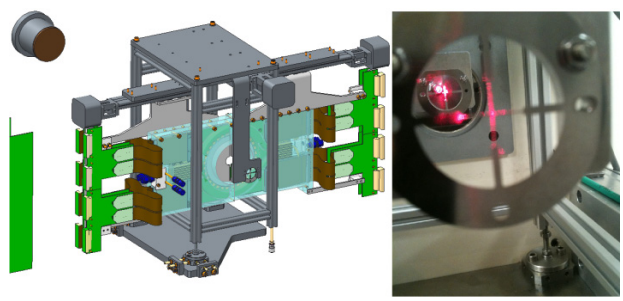

Figure 8: The stand alignment system consists of a laser boss sat on the beam line marking its centre and two cross-type targets for horizontal and vertical adjustment of the stand with respect to the beam line centre.

FARADAY CUP OPTIMISATION

In order to precisely monitor the absolute beam current, a FC optimised for the measurement of the 60 MeV treatment beam was also designed. It was important to optimise both, the beam stopper material and the geometrical arrangement to maximise the charge collection efficiency. These studies were performed with

ISBN 978-3-95450-127-4

the FLUKA Monte Carlo code [5]. Investigations into suitable materials and geometries focused on the minimisation of the proton-induced flux of various charged particles liberated from the surface of the beam stopper after impact of the 60 MeV proton beam [9]. These influence the overall charge collection efficiency and hence the performance of the monitor. Simulation studies showed that secondary electrons and protons escaping from the metal surface can cause significant measurement accuracy deterioration, see Table 1.

Despite graphite showing the lowest proton-induced charged particle currents, see Table 1, it was decided to choose Aluminium as material for the beam stopper due to its better mechanical properties. Low beam power of only P=0.3 W doesn't require any cooling [10]. Therefore it was possible to further simplify the FC geometry and a flat bottom shape was chosen.

Table 1: Charged Particle Currents From the FC as a Function of the Beam Stopper Material

Material	$I_{protons}$ [nA]	$I_{electrons}$ [nA]
Copper	$2.97 \cdot 10^{-5}$	$5.45 \cdot 10^{-4}$
Aluminium	$2.54 \cdot 10^{-5}$	$3.22 \cdot 10^{-4}$
Graphite	$2.54 \cdot 10^{-5}$	$3.38 \cdot 10^{-5}$

The FC was impedance matched to a 50 Ω SMA CF-based flange and a signal cable. CF type connections were chosen for the vacuum vessel. A HiPace80 turbo pump lowers the pressure in the vessel to $4.2 \cdot 10^{-6}$ mbar. A 50µm thick Kapton foil was chosen as the vacuum end window mounted on a VITON gasket. Its thickness was decided as a compromise between low beam energy losses and the required strength to withstand the pressure difference. The beam stopper is mounted directly on an end flange and isolated by a MACOR layer, see Fig. 9. The readout electronics consists of a FEMTO DHCPA-100 low noise amplifier and a GAGE RAZOR digitizer.

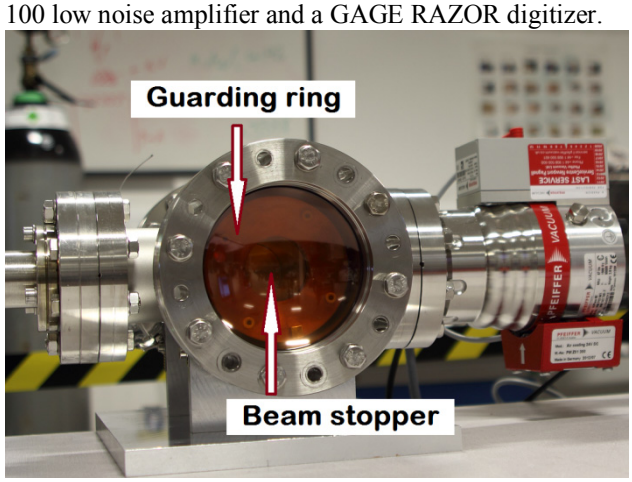

Figure 9: A flange-mounted Faraday Cup optimised for the 60MeV proton beam.

SUMMARY

A stand-alone test stand was designed to allow for the integration of the LHCb VELO detector into the treatment beam line at the Clatterbridge Cancer Centre. It is planned to use the detector as a new online, non–intrusive beam monitor, based on proton beam 'halo' detection. In its design it was crucial to guarantee safe operation of the detector in air, a remote controlled multi-axes positioning system, as well as integrate an efficient cooling system to avoid over-heating and minimize noise. The system is currently being commissioned and will be installed at the CCC for tests with beam in October 2013.

An Aluminium based Faraday cup was also designed, optimised and built for the characteristics of the proton beam at CCC. It will be used to precisely determine the absolute beam current. The LHCb VELO readings will then be related to these current readings and studies will be carried out to determine the sensitivity and reliability of signal cross correlation. Thereby, halo–current mappings will be determined that shall give access to an online dose monitoring during treatment. The shape of the FC beam stopper has been optimized in numerical simulations with FLUKA. Aluminium was chosen as absorber material for the collector electrode.

REFERENCES

[1] Beam emittance measurements and beam transport optimisation at the Clatterbridge Cancer Centre, Proc. IPAC 2013, MPOWA059, Shanghai 2013, http://jacow.org/.

[2] LHCb VELO Technical Design Report, CERN/LHCC 2001-0011, LHCb TDR 5, Geneva.

[3] A. Kacperek, 'Proton therapy of eye tumours in the UK: a review of the treatment at Clatterbridge, Applied Radiation and Isotopes 67, 378-386 (2009).

[4] G. Casse, a poster 'A LHCb VELO module as beam quality monitor for proton therapy beam at the Clatterbridge Centre for Oncology' University of Liverpool, *private communication*.

[5] A. Ferrari et al. 'FLUKA: a multi-particle transport code', CERN-2005-010, CERN, Geneva 2005.

[6] 'The LHCb Technical Design Report, Re-optimized Detector Design and Performance', LHCb TDR 9, CERN, Geneva 2003.

[7] 'The LHCb Detector at LHC', Journal of Instrumentation, Institute of Physics, 2008.

[8] EHS High Precision HV Modules, Operator's Manual, Rossendorf 2011.

[9] J.F. Janni et al., 'Proton Range – Energy Tables, 1keV – 10GeV: Energy Loss, Range, Path Length, Time-of-Flight, Straggling, Multiple Scattering, and Nuclear Interaction Probability', Atomic Data and Nuclear Data Tables No. 27, 147-339 (1982).

[10] P. Strehl, 'Beam Instrumentation and Diagnostics', Springer-Verlag Berlin Heidelberg 2006.

ISBN 978-3-95450-127-4